Measurement of laser intensities approaching 10^{15} W/cm^2 with an accuracy of 1%

M. G. Pullen,[1,2,*] W. C. Wallace,[1,2] D. E. Laban,[1,2] A. J. Palmer,[1,2] G. F. Hanne,[3] A. N. Grum-Grzhimailo,[4] K. Bartschat,[5]
I. Ivanov,[6] A. Kheifets,[6] D. Wells,[7] H. M. Quiney,[7] X. M. Tong,[8] I. V. Litvinyuk,[2] R. T. Sang,[1,2] and D. Kielpinski[1,2,†]

[1]*ARC Centre of Excellence for Coherent X-Ray Science, Griffith University, Nathan, Australia*
[2]*Australian Attosecond Science Facility and Centre for Quantum Dynamics, Griffith University, Nathan, Australia*
[3]*Atomic and Electronics Physics Group, Westfälische Wilhelms-Universität, D-48149 Münster, Germany*
[4]*Skobeltsyn Institute of Nuclear Physics, Lomonosov Moscow State University, Moscow 119234, Russia*
[5]*Department of Physics and Astronomy, Drake University, Des Moines, Iowa 50311, USA*
[6]*Research School of Physical Sciences, The Australian National University, Canberra, Australia*
[7]*ARC Centre of Excellence for Coherent X-Ray Science, University of Melbourne, Melbourne, Australia*
[8]*Division of Materials Science, Faculty of Pure and Applied Sciences, and Center for Computational Science, University of Tsukuba, 1-1-1
Tennodai, Tsukuba, Ibaraki 305-8577, Japan*

Accurate knowledge of the intensity of focused ultrashort laser pulses is crucial to the correct interpretation of experimental results in strong-field physics. We have developed a technique to measure laser intensities approaching 10^{15} W/cm^2 with an accuracy of 1%. This accuracy is achieved by comparing experimental photoelectron yields from atomic hydrogen with predictions from exact numerical solutions of the three-dimensional time-dependent Schrödinger equation. Our method can be extended to relativistic intensities and to the use of other atomic species.

I. INTRODUCTION

Strong-field laser experiments invoke highly nonlinear physical phenomena and are therefore, by their very nature, extremely sensitive to the exact value of the peak laser intensity. Phenomena such as above-threshold ionization (ATI) and high-harmonic generation (HHG) are widely used for a variety of applications. Retrieving accurate conclusions from these experiments typically relies on simulations incorporating a faithful reproduction of the experimental conditions. The peak laser intensity is a parameter that is vital to the correct retrieval of physical information from these experiments. The nonlinear nature of the processes is such that changes in the peak intensity of only a few percent can cause readily detectable changes in the electron and photon yields. Moreover, the value of the laser intensity is often only known at the order-of-magnitude level. Accurate approaches for determining this intensity are therefore required.

Initial methods for *in situ* intensity calibration were based upon the comparison of experimental single [1] and double [2] ionization rates to theoretical calculations. Recently, a number of novel methods to measure the intensity of pulsed lasers have been developed [3–5]. In particular, there are two *in situ* methods that can be considered the current state of the art. The first method, pioneered by Litvinyuk *et al.* [6] and subsequently improved upon by Alnaser *et al.* [7] and Smeenk *et al.* [8], compares theoretical simulations based upon the combination of ADK [9] ionization rates and classical mechanics to the photoelectron and photo-ion momentum distributions obtained from cold target recoil ion momentum spectroscopy (COLTRIMS) [6,7] and velocity map imaging

[8]. The second state of the art method was implemented by Micheau *et al.* [10] and Chen *et al.* [11]. It allows for the retrieval of multiple laser parameters via the comparison of high-energy photo-electron spectra to the recently developed quantitative rescattering theory [12]. While the accuracy of these methods is claimed to be at the 10% level, they both rely on theoretical models that employ significant approximations. The manner in which these simplifications affect the accuracy, as opposed to the precision, of the intensity measurement has not been addressed to date.

Here we use the energy-dependent photoelectron yield of atomic hydrogen (H) to calibrate the laser intensity at the 1% level. This is an order-of-magnitude improvement over the current state of the art. The experimental method we present essentially eliminates theoretical sources of inaccuracy since we are comparing experimental electron yields to highly accurate numerical results from three-dimensional (3D) time-dependent Schrödinger equation (TDSE) calculations. This renders our method virtually immune from systematic errors that might arise from theoretical approximations such as those used in previous reports. ATI spectra from atomic H have been studied previously with longer pulses [13]. A comparison to theoretical calculations was performed and qualitative agreement was found, however, the data were not exploited for quantitative analysis of laser parameters.

One familiar method of determining the peak intensity of a pulsed laser is by measuring the following set of observables: the average power (P), the pulse duration (t_p), the laser repetition rate (ν_R), and the $1/e^2$ Gaussian beam radius of the laser spot (w). These parameters can be combined to obtain the estimated laser intensity through

$$I_E = \frac{2P}{\pi w^2} \frac{1}{\nu_R t_p}, \tag{1}$$

where $P = U\nu_R$, with U as the pulse energy. The challenge faced by this method is the rapid accumulation of measurement

*Present address: Centre for Atom Optics and Ultrafast Spectroscopy, Swinburne University of Technology, Melbourne, Australia; mgpullen@gmail.com

†d.kielpinski@griffith.edu.au

TABLE I. Laser observables that are combined to form the laser intensity and their approximate measurement errors. Errors were derived using standard error propagation techniques and combined as the square root of the sum of the squares.

Observable	1σ error contribution
Laser power (P)	5%
Repetition rate (ν_R)	Negligible
Pulse duration (t_p)	5%
Beam waist (w)	$2 \times 5\%$
Total	10%

error. For this reason an uncertainty at the order-of-magnitude level is not uncommon. A typical error budget for the laser observables outlined above is summarized in Table I. The budget is usually dominated by the error in determining w due to the limitations of typical beam profiling devices in imaging focused beams. (The fractional error of w is doubled due to the $I \propto 1/w^2$ dependence.)

The measurement method presented in this work compares experimental ATI yields obtained from the interaction of atomic H with a few-cycle laser ($t_p \sim 6.3$ fs) to the predictions from two 3D TDSE implementations. In addition to the two 3D TDSE simulations we have included three other common theoretical implementations as a comparison to show that exact numerical solutions of the 3D TDSE are required in order to accurately measure the laser intensity. With the inclusion of focal-volume integration and a detailed understanding of the detection system, a quantitative comparison of the experimental data to each set of theoretical simulations becomes possible. The results show that an intensity measurement accuracy at the 1% level has been achieved which is an order-of-magnitude improvement over the current state of the art. The present method also has the potential to be used as an intensity calibration tool for experimental systems where the calculations require the use of approximations, such as in typical high-harmonic generation and ATI experiments and in relativistic laser physics.

II. EXPERIMENTAL DETAILS

The apparatus and the data acquisition method used in this work have been described elsewhere [14,15] and thus are only summarized briefly here. An atomic H beam is intersected with a focused and linearly polarized few-cycle laser beam. The yield of photoelectrons ($\sim 10^4$ laser pulses per data point) is detected as a function of energy. The electron detection system is composed of a stack of electron lenses and a channel electron multiplier. A "deflection" voltage (V_D) is applied to the electron lens stack with the effect of repelling electrons below some cutoff energy. In this way, V_D can be varied so that energy-resolved electron spectra can be obtained. The components used in this detection system are simple and very well understood. As such, our detection system is much less complicated than systems such as typical time-of-flight spectrometers, velocity map imaging, and COLTRIMS and, thus, allows the response of the system to be accurately simulated using the SIMION modeling package [16] so that

the trajectory of the ionized electrons can be determined as a function of V_D.

The laser used in the experiments present here is derived from a commercial Femtolasers product and is centered at 800 nm with a repetition rate of 1 kHz. The pulse duration was measured to be 6.3 fs multiple times during data acquisition using a commercial few-cycle autocorrelator. The signals of the wings of the autocorrelation trace were typically about 10%–15% of the main pulse. In addition, no signal above noise was observed for autocorrelation times greater than about 10 fs either side of the main peak. This indicates that our most conservative estimate would give a pre or post pulse with an upper limit of its energy at 10%–15% of the main pulse and an upper limit of its temporal extent of about 10 fs. As will be seen, even if a small pre or post pulse were present, the results indicate that it does not affect the ability of the system to accurately measure the peak laser intensity. The laser intensity can be varied between 1×10^4 and 5×10^{14} W/cm^2 by inserting pellicle beamsplitters, which have a negligible effect on the pulse duration. The experimental results obtained consist of nine data sets ($n = 1, \ldots, 9$), each with a detected electron yield as a function of V_D for a different laser intensity. Two of the data sets were taken using a similar intensity in order to show reproducibility.

III. THEORETICAL IMPLEMENTATIONS

We compare to a wide variety of theoretical methods with different levels of approximation. In order, roughly speaking, from most exact to least exact, the methods are as follows: two independent numerical solutions of the 3D TDSE, by Grum-Grzhimailo *et al.* [17] and Ivanov [18], which both use the velocity gauge and which give identical outputs for identical inputs; a pseudospectral method that utilizes the integral form of the 3D TDSE rather than the differential form and is in the length gauge [19]; a one-dimensional (1D) solution of the TDSE in the velocity gauge; and a semiclassical method that follows the method presented by Keldysh [20], in which a Volkov wave function is used in the velocity gauge of the interaction Hamiltonian. The pulse duration used in all simulations is 6.3 fs at full width half-maximum (FWHM), except for the pseudospectral method and the 3D TDSE solution based on the work of Ivanov [18], where pulse durations of 5.5 fs at FWHM were used. It should be noted that agreement to within $<1\%$ has been shown between the two 3D TDSE solutions when the exact same input parameters were used. We can therefore be sure that any differences between the results of the two can be attributed to the change in the pulse duration only and are not due to the small differences in the numerical techniques implemented. The comparison of the experimental data with the solutions of the 3D TDSE for two pulse durations serves as an excellent way to test the sensitivity of our method to the exact value of the pulse duration at the experiment.

Each theoretical approach provides the photoelectron yield as a differential ionization rate with respect to the electron energy (E) and the angle from the laser polarization direction (θ). The differential ionization rate can then be written as $dP(E,\theta)/d\theta dE$. The ionization rates are expressed in units of eV^{-1} sr^{-1} and are calculated for 14 values of laser peak

intensity between $0.58.0 \times 10^{14}$ W/cm^2. A central wavelength of 800 nm, corresponding to a photon energy of 1.55 eV, was used in all simulations except the pseudospectral method where a wavelength of 750 nm was used. The difference in wavelength for the pseudospectral method is far less than the 200-nm FWHM spectral bandwidth of the laser, so the induced error should be negligible. Most of the simulations are computationally expensive and only a single suitable set of theoretical simulations was available for each model. In no way were the input parameters tweaked to fit the results. As the laser carrier envelope phase (CEP) was not stabilized in the present experiments, the predicted differential ionization rates were averaged over 12 values of the CEP covering the full 2π range. Preliminary CEP-resolved experimental results, which are not presented in this paper, indicate that the maximum modulation caused by a change in the CEP is of the order of 10%. As the electron yields in this paper are integrated over 10^4 laser pulses, each with essentially a random CEP value, the expected error due to averaging over CEP is $10\%/\sqrt{10^4} = 0.1\%$, which is negligible.

IV. COMPARISON OF EXPERIMENT AND THEORY

Neglecting the spatial variation of the laser beam, the total ionization rate for a constant peak intensity can be expressed as

$$P(V_D, I_P) = 2\pi \int \frac{dP(E,\theta,I)}{dEd\theta} f(E,\theta,V_D) \sin\theta \, d\theta \, dE. \quad (2)$$

Here $f(E,\theta,V_D)$ term is the acceptance function of the detection system, which is derived from SIMION simulations of electron trajectories in the detector.

The issue of focal volume averaging in the context of retrieving the peak intensity of a laser is very important. Contributions to the detected electron yields due to the extended spatial profile of the focused beam are significant and must be accounted for. Failure to include these contributions results in an unsatisfactory comparison of experimental data with theoretical simulations. We can model the transverse beam profile of the laser using a Gaussian fit function,

$$I(r,z) \sim I_P e^{-2r^2/w(z)^2}, \quad (3)$$

where r and z are the transverse and axial directions, respectively, $w(z)$ is the laser waist radius along z, and I_P is the peak laser intensity. Using a Gaussian fit function is justified in this experiment, as measurements have shown that propagation of the laser is only slightly off being ideal with $M^2 \sim 1.5$. The width of the interaction region is defined by two pinhole apertures and is about $d = 0.5$ mm. As our laser is loosely focused, a distance of 0.5 mm is small enough that beam propagation effects can be ignored. In this case, the interaction volume can be approximated as a cylinder of length d and radius w while introducing a $<0.1\%$ error in the calculated volume. A scan of the focal region was performed using a commercial CCD beam profiler in order to confirm that the focused laser beam was not suffering from any aberrations such as astigmatism.

Combining Eqs. (2) and (3) and integrating over the focal volume, we arrive at the total electron yield as a function of

I_P and V_D:

$$S(V_D, I_P) \propto \int_0^\infty P(V_D, I_P e^{-2r^2/w^2}) r \, dr. \quad (4)$$

The task of the present work is to determine the value of I_P by fitting the experimental data to theory, thus calibrating the laser intensity. As the first test of the theoretical models, we compare the values of I_P, which were obtained by fitting the nine data sets to theory, with the values obtained by measuring the laser observables. The values obtained from laser measurements, denoted $I_{E,n}$, for $n = 1, \ldots, 9$, are only precise at the 10% level. However, the relative error between these measurements is much smaller, arising only from the 5% error in the power meter measurement.

Any theory that is suitable for use in intensity calibration should therefore yield best-fit values $I_{P,n}$ that differ from the $I_{E,n}$ results only by a multiplicative rescaling factor of the electron yield S that is the same for all nine data sets. The comparison between $I_{P,n}$ and $I_{E,n}$ is achieved by performing a global weighted [21] least-squares fit of the experimental data sets with each theoretical data set. We use only two parameters for this global fit. First, the parameter η provides an overall multiplicative rescaling of the intensity, $\eta = I_{P,n}/I_{E,n}$. If a theory is adequate for intensity calibration, $I_{P,n}$ should only depend on η and $I_{E,n}$. Second, the common multiplicative rescaling of the electron yield S to account for the unknown atomic density and detector efficiency.

V. DISCUSSION

The results of the global fit are presented in Fig. 1(a) for one representative experimental data set only. The detected electron yield is shown as a function of the electron cutoff energy defined by the voltage applied to the electron lens stack. Results for the other data sets are similar and are presented in the Supplementary Information [22]. The estimated laser intensity used for this data set is $I_{E,7} = (4.5 \pm 0.5) \times 10^{14}$ W/cm^2. The experimental data are shown together with the 6.3-fs 3D TDSE fit (solid line), the 5.5 fs 3D TDSE fit (dotted line), the pseudospectral fit (dashed-dotted line), the 1D TDSE fit (long-dashed line), and the semi-classical fit (short-dashed line). Interestingly, the fit of the 6.3-fs 3D TDSE simulation is statistically identical to the fits of the 5.5-fs 3D TDSE and the 6.3-fs pseudospectral methods. The value of η for each theoretical method is shown in the legend.

The fits of the two independently calculated 3D TDSE calculations exhibit very good agreement with the experimental data. The value of the intensity scaling fitting parameter is $\eta = 0.93 \pm 0.02$ for both. This suggests that, on average, we overestimated the laser intensity by $\sim 7\%$ when measuring the laser observables. The cause of this systematic overestimation is probably due to the inaccurate calibration of the CCD beam profiler used to measure the focused spot size. The value of $\eta = 1.08 \pm 0.02$ for the pseudospectral method, on the other hand, is significantly different from the two 3D TDSE methods. This indicates that while the pseudospectral method can correctly fit the experimental electron yield data, it systematically underestimates the actual laser intensity. Similarly, the 1D TDSE and the semiclassical fits also underestimate the actual intensity by 8% and 32%, respectively. In addition, both
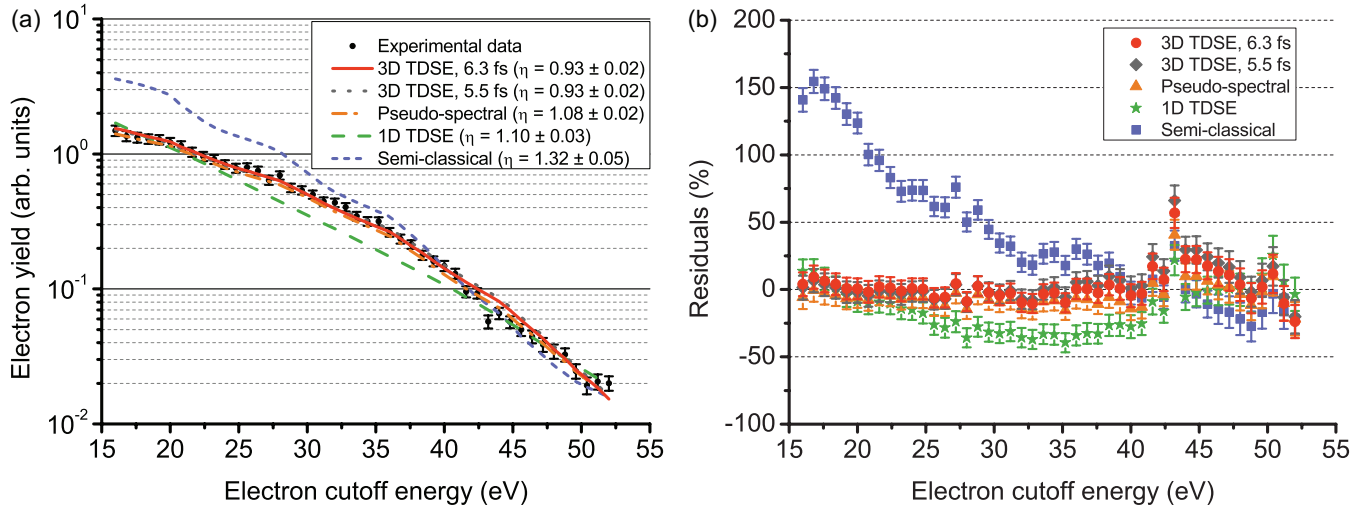
FIG. 1. (Color online) (a) Detected photoelectron yield as a function of the electron cutoff energy. Experimental data are shown with the results of the global fitting routine. The value of η for each theoretical method is shown in the legend. (b) Residuals of the fits to the data shown in (a). It is important to note that fit of the 6.3-fs 3D TDSE simulation (performed by Grum-Grzhimailo *et al.* [17]) is statistically identical to the fits of the 5.5-fs 3D TDSE (performed by Ivanov [18]) and the 6.3-fs pseudospectral (performed by Tong *et al.* [19]) methods in both (a) and (b).

theories yield poor fits to the data, thus failing the test of accuracy set by the 10% error in $I_{E,n}$.

The agreement of the different theory fits to the experimental data is presented in Fig. 1(b) as percentage residuals. The residuals of the 6.3-fs 3D TDSE fit (circles) are close to 0 for the entire data set, whereas the residuals of the 1D TDSE (stars) and the semiclassical (squares) methods are much larger. Again, the residuals of the 5.5-fs 3D TDSE (diamonds) and the pseudospectral (triangles) completely overlap with the 6.3-fs 3D TDSE residuals. It is important to note that the general behavior of the residuals is similar for the other eight data sets used in the global fit as shown in the Supplementary Information [22]. The data point near 43 eV can be considered a statistical outlier, which is not unexpected for a data set which includes >50 data points. The statistical fluctuation could have been driven by short-term deviations in the laser intensity or the gas density at the interaction region, for example.

We can extend the fitting routine by replacing η with an intensity scaling fitting parameter for each of the n different data sets such that $\eta_n = I_{P,n}/I_{E,n}$. This allows for the predicted intensities to be shifted relative to each other and thus produces a much more accurate method of determining the individual laser intensities used in each data set. As an example, an intensity of $I_{P,7} = (4.08 \pm 0.03) \times 10^{14}$ W/cm^2 is obtained for the experimental data shown in Fig. 1 when this extended fitting routine is implemented with the 6.3-fs 3D TDSE calculations. The error in I_P is more than a factor of 10 smaller than the error in I_E. It corresponds to a measurement accuracy of <1%, which is an order-of-magnitude improvement over previous methods.

The results of the extended fitting routine for each of the theoretical implementations are presented in Fig. 2 as percentage differences from the 6.3-fs 3D TDSE predictions. Each data point represents the estimated laser intensity for one of the nine data sets. The predictions of the different theoretical implementations are shown in by different shapes: 6.3-fs 3D

TDSE (circles), 5.5-fs 3D TDSE (diamonds), pseudospectral (triangles), 1D TDSE (stars), and semiclassical (squares). The shaded area corresponds to the experimental error in determining I_E and is shifted vertically by $\sim$7% to account for the systematic error for all of the $I_{E,n}$ values, as discussed above.

The percentage difference of the 5.5-fs 3D TDSE is 0 within error for all data sets. This shows that our experimental method is insensitive to the exact value of the pulse duration. This would be extremely useful on occasions when the pulse duration at the interaction region cannot be determined accurately.
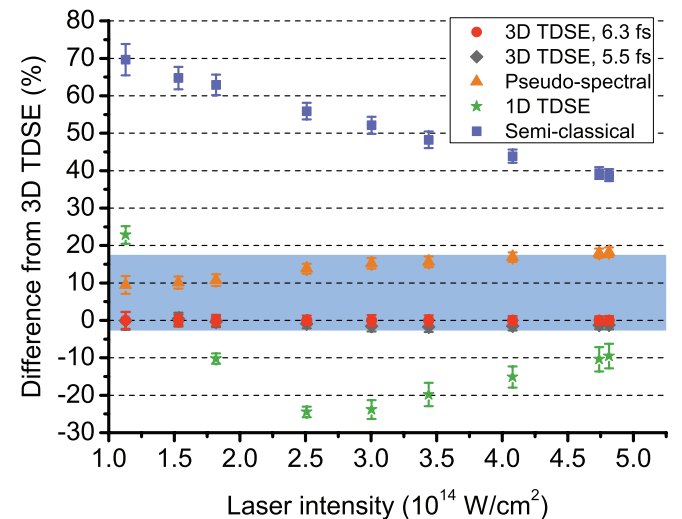

FIG. 2. (Color online) Results of the theoretical predictions from the extended fitting routine are shown as percentage differences from the 6.3-fs 3D TDSE predictions. The shaded area corresponds to the typical $\pm$10% experimental error in determining I_E as outlined in Table I. It has also been shifted vertically by $\sim$7% due to the systematic overestimation of I_E as described in the text.

This observation indicates that our method is actually sensitive to the peak intensity rather than the pulse energy. If the method was, instead, more sensitive to pulse energy, the retrieved peak intensity would have a clear dependence on pulse duration.

There are two points worth mentioning regarding the predictions of the 1D TDSE model and the semiclassical approach. Both sets are inconsistent with power meter measurements over the entire intensity range, and their systematic errors vary with the laser intensity. Applying a constant correction factor, therefore, would still not make either of the implementations suitable for intensity calibration. The presented results confirm that both the 1D TDSE and the semiclassical results should only be used for qualitative comparison, and not for a quantitative analysis. It is clear from these results that these two theoretical methods are unsuitable for accurate intensity determination by photoelectron yield measurements. In the case of the 1D TDSE, it is perhaps not unexpected that the simulations do not follow experiments, as low-energy electrons in ATI are not necessarily ejected parallel to the laser electric field [23].

Interestingly, the pseudospectral predictions fall close to the 3D TDSE results for all laser intensities investigated in this work, and almost all of them are consistent with the measurements based on laser observables. Perhaps it is not unexpected that this method performs closest to the 3D TDSE models, as it is also quite successful at fitting the raw electron yields. The accuracy of this method is due to the fact that it uses an exact numerical solution to the 3D TDSE within a certain distance from the core and invokes an approximation only outside of that range. However, given that we are unable to resolve the systematic shift of the pseudospectral predictions by measuring the laser observables, this suggests that extreme care must be taken when using any intensity measurement scheme which does not utilize full numerical integration of the 3D TDSE. While the fitting errors of measurement techniques based on theoretical approximations may well be of the order of a few percent, there might be systematic errors present that are closer to tens of percents.

In using our intensity calibration technique, it is not required that atomic H and another target gas should be delivered through the same source. In fact, the most useful and realistic implementation would have the sources separated. This would allow a measurement of the peak intensity on demand. In addition, the density requirements of the technique presented here are orders of magnitude lower than the gas sources used in most high-field physics experiments such as gas jets and gas cells. This means that the atomic H source can be well separated from the interaction region so that it does not interfere with experiments involving other gases.

In future work, we plan to obtain calibration data that can be used in other laboratories without access to atomic H. This could be implemented as follows: The photoelectron spectra of atomic H and other gas species of interest can be measured for a wide range of laser intensities and electron energies using the same apparatus and laser parameters. A unique calibration curve can be obtained for each target species by comparing the measured electron spectra to that of atomic H. If these calibration curves are available to all researchers, an accurate value of the peak laser intensity at the interaction region may be obtained in any experiment by comparing the measured electron spectrum to the predetermined calibration curve. The issue of focal-volume averaging, of course, complicates matters, as some high-field experiments use gas jets of non-negligible thickness, and hence laser propagation effects cannot be neglected. This issue will be addressed in future work.

VI. CONCLUSION

We have presented a method for measuring the peak intensity of high-field laser pulses with an accuracy of 1%, which is an order-of-magnitude improvement over the current state of the art. This unprecedented accuracy is due entirely to the direct comparison of exact numerical solutions of the 3D TDSE to experimental electron yields from atomic hydrogen. In contrast, invoking any theoretical approximations leads to easily detectable inaccuracy in the retrieved laser intensity. This result highlights the need to evaluate the error arising from theoretical approximations in other laser intensity measurement results which have relied on approximate theoretical methods. Our method removes the ambiguities that are inherent in previous intensity measurement schemes and has applications in current high-field research areas such as attosecond science and relativistic laser physics. The technique can, in principle, be used to calibrate the peak laser intensity for any high-field experiment where the photoelectron spectrum can be measured.

[1] S. F. J. Larochelle, A. Talebpour, and S. L. Chin, J. Phys. B: At. Mol. Opt. Phys. **31**, 1215 (1998).

[2] V. R. Bhardwaj, S. A. Aseyev, M. Mehendale, G. L. Yudin, D. M. Villeneuve, D. M. Rayner, M. Yu. Ivanov, and P. B. Corkum, Phys. Rev. Lett. **86**, 3522 (2001).

[3] R. Wiehle, B. Witzel, H. Helm, and E. Cormier, Phys. Rev. A **67**, 063405 (2003).

[4] Y. Wang, J. Zhang, Z. Xu, Y. S. Wu, J. T. Wang, and D. S. Guo, Phys. Rev. A **80**, 053417 (2009).

[5] S. Xu, X. Sun, B. Zeng, W. Chu, J. Zhao, W. Liu, Y. Cheng, Z. Xu, and S. L. Chin, Opt. Express **20**, 299 (2011).

[6] I. V. Litvinyuk, K. F. Lee, P. W. Dooley, D. M. Rayner, D. M. Villeneuve, and P. B. Corkum, Phys. Rev. Lett. **90**, 233003 (2003).

[7] A. S. Alnaser, X. M. Tong, T. Osipov, S. Voss, C. M. Maharjan, B. Shan, Z. Chang, and C. L. Cocke, Phys. Rev. A **70**, 023413 (2004).

[8] C. Smeenk, J. Z. Salvail, L. Arissian, P. B. Corkum, C. T. Hebeisen, and A. Staudte, Opt. Express **19**, 9336 (2011).

[9] M. V. Ammosov, N. B. Delone, and V. P. Kraǐnov, Zh. Eksp. Teor. Fiz. **91**, 2008 (1986) [Sov. Phys. JETP **64**, 1191 (1986)].

[10] S. Micheau, Z. Chen, A. T. Le, J. Rauschenberger, M. F. Kling, and C. D. Lin, Phys. Rev. Lett. **102**, 073001 (2009).

[11] Z. Chen, T. Wittmann, B. Horvath, and C. D. Lin, Phys. Rev. A **80**, 061402(R) (2009).

[12] Z. Chen, A. T. Le, T. Morishita, and C. D. Lin, Phys. Rev. A **79**, 033409 (2009).

[13] G. G. Paulus, W. Nicklich, F. Zacher, P. Lambropoulos, and H. Walther, J. Phys. B: At. Mol. Opt. Phys. **29**, L249 (1996).

[14] M. G. Pullen, W. C. Wallace, D. E. Laban, A. J. Palmer, G. F. Hanne, A. N. Grum-Grzhimailo, B. Abeln, K. Bartschat, D. Weflen, I. A. Ivanov, A. Kheifets, H. M. Quiney, I. V. Litvinyuk, R. T. Sang, and D. Kielpinski, Opt. Lett. **36**, 3660 (2011).

[15] W. C. Wallace, M. G. Pullen, D. E. Laban, O. Ghafur, H. Xu, A. J. Palmer, G. F. Hanne, K. Bartschat, A. N. Grum-Grzhimailo, H. M. Quiney, I. V. Litvinyuk, R. T. Sang, and D. Kielpinski, New J. Phys. **15**, 033002 (2013).

[16] Available at: http://www.simion.com/.

[17] A. N. Grum-Grzhimailo, B. Abeln, K. Bartschat, D. Weflen, and T. Urness, Phys. Rev. A **81**, 043408 (2010).

[18] I. A. Ivanov, Phys. Rev. A **83**, 023421 (2011).

[19] X. M. Tong, K. Hino, and N. Toshima, Phys. Rev. A **74**, 031405(R) (2006).

[20] L. V. Keldysh, Sov. Phys. JETP **20**, 1307 (1964).

[21] The weights here are experimental error bars that include contributions from shot noise, dissociation fraction error, and Allan deviation analysis as described in [14].

[22] See Supplemental Material at http://link.aps.org/supplemental/10.1103/PhysRevA.87.053411 for all nine data sets used in the global fit.

[23] W. Becker, A. Lohr, and M. Kleber, J. Phys. B **27**, L325 (1994).